Theor Chem Acc (2009) 123:501–511
DOI 10.1007/s00214-009-0570-8

REGULAR ARTICLE

Is high electric field capable of selectively inducing a covalent-like bond between polar and non-polar molecular species?

Dhurba Rai · Anant D. Kulkarni · Shridhar P. Gejji · Rajeev K. Pathak

Received: 17 March 2009 / Accepted: 10 April 2009 / Published online: 15 May 2009

Abstract It is demonstrated through the present ab initio theoretical investigation that an external electric field can bring about a phenomenal enhancement in the strength of the bond between water and carbon-dioxide molecules from a van der Waals type (binding energy $\sim$0.085 eV), to strong covalent type (binding energy $\sim$7.45 eV), resulting in an exotic molecular complex. The onset of this effect is characterized by an abrupt change in the dipole moment of the composite system at a particular field-value, concomitant with the O–C=O $\leftrightarrow$ O=C–O resonance in the CO_2 moiety of the complex. This field-induced bond formation is further confirmed by the emergence of a characteristic intermolecular stretching mode ($\sim$317 cm^{-1}) in the vibrational response of the system. This exotic bond that exhibits a covalent-like character, which accompanied by a charge-transfer, renders the carbon atom a substantial negative charge.

D. Rai · R. K. Pathak (✉)
Department of Physics, University of Pune,
Pune 411007, Maharashtra, India
e-mail: pathak@physics.unipune.ernet.in

A. D. Kulkarni · S. P. Gejji
Department of Chemistry, University of Pune,
Pune 411007, Maharashtra, India

Present Address:
A. D. Kulkarni
Department of Petroleum and Chemical Engineering,
University of Pittsburgh, Pittsburgh, PA 15261, USA

1 Introduction

Polar molecules, such as H_2O, HX (X=F, Cl, Br, I, etc.), H_2O_2, C_6H_5F, NH_3, by virtue of their electric dipole moments interact weakly to form bound molecular complexes, a well-known instance being intermolecular hydrogen bonding [1–8]. Non-polar molecules on the other hand, form extremely weakly bound agglomerates with polar or non-polar species by hydrogen bonding or by induction of small dipole moments through van der Waals interaction [1–8]; e.g. $C_2H_2\cdots H_2O$ (with the acetylene molecule always linear), $CO_2\cdots HF$ (nearly linear geometry) $H_2S{\cdot}CO_2$ (nearly perpendicular molecular planes), and $H_2O{\cdot}CO_2$ (almost planar).

To bring about significant structural changes and charge redistribution in such weakly interacting systems without introduction of any additional reactants, a stimulus such as a sufficiently high external electric field is required [9–11]. For example, in the $ClH\cdots NH_3$ complex [11], a field applied along the traditional H···N hydrogen bond, first converts it into a proton-shared Cl···H···N hydrogen bond, and subsequently enforces the proton transfer resulting in a hydrogen bonded ion pair, a mechanism that is a prototype for proton transfer in crystals [12–14]. Recent years have witnessed a surge of activity investigating responses of molecular systems as well as complexes to applied static electric fields [9–15]. Albeit sustained over distances of only a few Bohr radii (a_0, the Bohr radius $\sim$0.529 Å), electric field strengths at the molecular level can be extremely high: the atomic unit of electric field being $\frac{|e|}{4\pi\varepsilon_0 a_0^2} = 5.142 \times 10^{11}$ V/m; even 0.2% of which becomes the order of a gigavolt per meter. Electric fields of this enormous magnitude actually manifest in molecular circuits with modest bias voltages [16–18], zeolite [19] or protein cavities [20, 21], active enzyme sites [22], as well

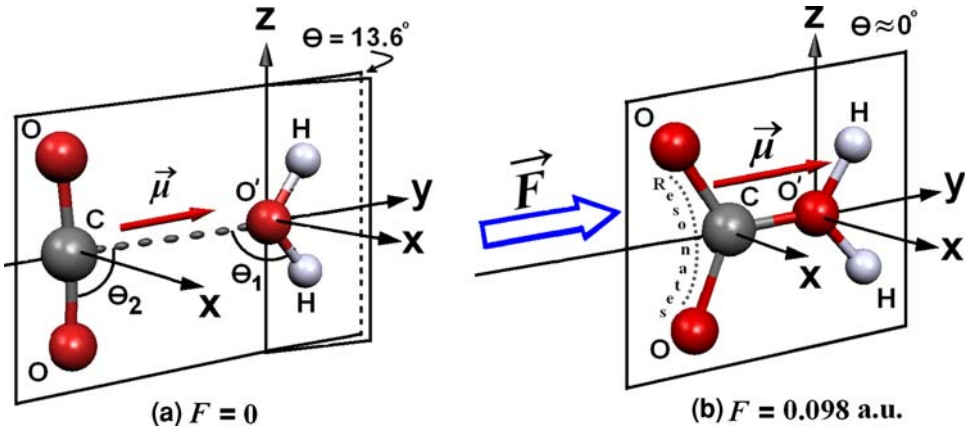

Fig. 1 Weakly bound, nearly planar T-shaped $H_2O'{\cdot}CO_2$ complex converted into an exotic, covalent-like bonded, practically planar molecular entity in the presence of externally applied electric field $\vec{F}$. (Oxygen of H_2O, is primed for distinction)

as between the probing tip and a conducting substrate in scanning tunneling microscopy [23]. Such high ambient electric fields can produce substantial molecular vibrational Stark shifts [24–26]. Several studies carried out hitherto primarily focus on electric fields applied to isolated molecules, or molecular complexes with polar constituents, bonded together either by dispersive forces (van der Waals interactions), or hydrogen bonding [27–29]. While we confine here to high but uniform and static fields in the present study, it must be noted that there exists a related theme of laser–molecule interactions, where molecules are subjected to intense dynamic electric fields of the laser. Bandrauk et al. [30] brought out the effect of absolute laser phase in laser induced chemical reactions and its ramifications. These authors found that in general dipole moments and polarizabilities exhibit extrema in the neighborhood of a transition state. They conclusively demonstrated that in fact larger dipole moments could lead to the creation of deep wells with new strongly bound states in the transition state region. Further, Uzer et al. [31], on the other hand, applied tenets of dynamical systems to a chemical reaction, through a suitable reaction coordinate and extracted time-dependent invariant manifolds emerging as separatrices between reactive and non-reactive trajectories. Employing a driven Hénon–Heiles system with a two-dimensional harmonic oscillator with additional nonlinear cubic couplings subject to an electric field with a spatially Gaussian profile, they generalized the transition state theory to driven systems enabling control of chemical reactions through laser pulses.

A very interesting and extremely relevant work by Matta et al. [32] very recently demonstrated that for a 'polar + polar' HF···HF dimer, the applied electric field strengthens the interaction due to a larger mutual polarization between both the molecules and *enhances the covalent character* of the hydrogen bond. In the present work, we demonstrate that this holds good for a selected pair of *non-polar* and *polar* molecules as well.

2 Field-enhanced molecular bonding

We bring out a remarkable effect induced by an applied external electric field $(\vec{F})$ on the otherwise a rather feebly interacting system of H_2O, a polar molecule (μ, the dipole moment = 1.85 D) and CO_2, a non-polar species in its free state. The $H_2O'{\cdot}CO_2$ complex, under normal conditions could be (i) a hydrogen-bonded species, or (ii) a planar [33] or (iii) a nearly planar van der Waals complex between the partially positive carbon atom and the partially negative oxygen of water (denoted by O′, primed for distinction). Energetically the global minimum is the third one, nearly planar, T-shaped structure [6, 34, 35] (Fig. 1a) with a shallow binding of 1.97 kcal mol^{-1} ($\sim$85 meV/molecule). For gaseous CO_2 (in the absence of any field), significant geometry distortion in terms of OCO bending is accomplished only when subjected to extremely high pressures and temperatures [36, 37]; where a fraction of it dimerizes [38].

We investigate field effects on the present polar–non-polar molecular complex, within the premise of the density functional theory (DFT) using the B3LYP [39, 40] prescription for the exchange-correlation functional integrated with the Gaussian-03 suite of programs [41]. In the presence of an externally applied electric field, the B3LYP level is a respectable level of theory that permits a full optimization of structures under Gaussian-03. All calculations are carried out by optimizing the geometry of the complexes in the presence of uniform static dipolar field using the split valence, triple zeta basis set augmented with diffuse and polarization function viz. 6-311++G(2d,2p), followed by a vibrational frequency calculation to confirm local minimality.

A uniform static field applied from zero, in steps of 0.001 a.u. along the net electric dipole moment of the equilibrium tilted (by 90° on its left side) 'T'-shaped structure is considered. The applied field induces an electric dipole moment in the otherwise non-polar CO_2

enhancing the dipole–dipole interaction between the species with a steady increase in field strength from zero up to 0.098 a.u. Above the field strength of 0.050 a.u. the C_{2v} axis of water in the complex aligns along the field direction rendering the structure planar, accompanied by a significant modification in the CO_2 geometry where the otherwise linear dioxide molecule distorts into a V-shaped structure with the oxygen atoms pointing away from hydrogen atoms of water (*cf.* Fig. 1). It must be noted that for an isolated molecule or weakly bound complexes the electric field invariably tends to dilate the structure by stretching the bond(s) [15, 27, 29]. In the present case, however, a major contraction of the bond results: the field compresses the C–O′ bond, bringing the molecules in closer encounter, consequently the two molecules get bonded: the 2.863 Å C–O′ distance at zero field, compresses to *nearly half this value*, to 1.442 Å at the maximum 'threshold' field strength of 0.098 a.u. Further increase in field diminishes this distance to a level where inter-nuclear Coulomb-repulsion dominates and the complex tends to dissociate. The structural parameters of equilibrium geometry in the absence of external electric field are given in Table 1 with their changes brought about by the field presented in Table 2. A particularly striking feature is that the C–O′ distance initially decreases steadily, but at the 0.040 a.u. field, there is drastic decrease, to a value of 1.781 Å accompanied by an abrupt change in the electric dipole moment of the complex. Subsequently, there is once again a steady decrease with increasing field, up to 0.098 a.u., the permissible threshold maximum. For a continuous medium it is customary to describe the response of a system subjected to an external electric field in terms of response functions (polarizability, electric susceptibility, etc.) that are decomposed into linear, quadratic (with the external field) and higher order contributions. It is to be noted that for the present case of a binary molecular complex, all effects—linear as well as nonlinear—are incorporated self-consistently.

Energetics directly brings out the effect of induced bonding: while the field-free total energy of the complex is –265.116 Hartree a.u.; the complex essentially gets increasingly stabilized by the electric field, as the following trend indicates: for field values, in a.u., of 0.040, 0.050, 0.080, and 0.098 (threshold maximum) the respective relative energies in kcal mol^{-1} are as follows: −40.656, −65.279, −164.802, and −246.655. For a given value of the electric field, the quantity ΔE, defined by $\Delta E \equiv$ total energy of the complex optimized at that value of the field—the sum of the energies of the molecular subunits with their geometries in the presence of the same field but 'frozen' to their respective field-optimized configurations in the complex, turns out to be—172.0 kcal mol^{-1}. As the major interaction between the dioxide and water is mediated by the C and O′ partners, this leads to an estimation of the bond energy $\sim$172.0 kcal mol^{-1} ($\sim$7.45 eV). For comparison, analogous study on the field-free CO_2 molecule, by varying one of the C=O distances, yields a value of 193.9 kcal mol^{-1} for the bond energy; which confirms that the C and O′ atoms that mediate the interaction, actually establish an appreciably strong covalent-type bond by virtue of considerable electron density migrating from the dioxide to the region amidst C and O′. The electric field thus renders the weak van der Waals type bond into an *over*-87-*times* stronger covalent-type bond. Incidentally, the process being reversible, the original weakly bound complex is recovered on reducing the applied field strength gradually to zero, precluding any 'hysteresis'. It must be noted that the present effect is not simply a minor structural

Table 1 The field-free equilibrium bond lengths (in Å), bond angles (in degrees), and the electric dipole moment (in Debye) of the $H_2O'{\cdot}CO_2$ complex calculated at the DFT (B3LYP) level of theory with the 6–311++G(2d,2p) basis set

Structure	CO (Å)	O′H (Å)	O···H (Å)	C·O′[a] (Å)	∠HO′H (°)	∠OCO (°)	Θ[b] (°)	Θ_1 (°)	Θ_2 (°)	μ (D)
Nearly planar	1.160	0.961	–	2.863	105.7	178.2	13.6	125.9	90.9	2.25
	1.168[c]	0.959[c]		2.771[c]	104.1[c]	178.0[c]	14.6[c]			
Planar	1.160	0.961	–	2.867	105.7	178.0	0	127.1	90.9	2.26
	1.170[d]	0.961[d]		2.800[d]	104.3[d]				90.8[d]	1.85[e]
				2.836[e]						
H-bonded	1.163[f]	0.962[f]	2.216	–	105.3	179.3	–	–	–	1.89
	1.158	0.960								

[a] C·O′ separation

[b] Angle with which the H_2O plane is inclined with respect to the CO_2 plane

[c] Calculated at MP2/6–31++G(d,p) level [6]

[d] Calculated at MP2/aug-cc-PVTZ + BSSE corrected level [35]

[e] Experimental value [33]

[f] Bond engaged in H-bonding and the other values in the next row are corresponding to the bonds not involved in H-bonding

Table 2 Bond distances (in Å) and bond angles along with dipole moments (in Debye) of the $H_2O'{\cdot}CO_2$ complex as a function of field-strength calculated at B3LYP level employing the 6–311++G(2d,2p) basis set

Electric field (in a.u.)	CO (Å)	O′H (Å)	C·O′[a] (Å)	∠HO′H (°)	∠OCO (°)	Θ_1 (°)	Θ_2 (°)	μ (D)
0.000	1.160	0.961	2.867	105.7	178.2	127.1	90.9	2.26
0.010	1.161	0.962	2.754	104.6	175.4	127.6	92.2	2.96
0.020	1.162	0.965	2.613	103.6	171.9	128.1	94.0	3.86
0.030	1.166	0.967	2.401	103.2	166.0	128.3	96.9	4.87
0.040	1.197	0.976	1.781	109.2	144.5	125.3	107.7	8.60
0.044	1.210	0.980	1.652	110.7	139.3	124.6	110.3	9.83
0.050	1.220	0.986	1.576	111.1	135.6	124.4	112.1	10.97
0.060	1.232	0.995	1.516	110.2	131.6	124.8	114.1	12.56
0.070	1.243	1.007	1.480	108.8	128.7	125.5	115.6	14.21
0.080	1.253	1.021	1.457	107.0	126.6	126.4	116.6	16.16
0.090	1.261	1.039	1.443	105.0	125.5	127.4	117.2	18.61
0.098	1.266	1.060	1.442	103.2	125.7	128.3	117.1	20.97

[a] Distance between O′, the oxygen of H_2O' and C, the carbon of CO_2

distortion caused by the field, but is essentially a field-induced covalent-like bonding, yielding an exotic, stable molecular entity which radically differs from H_2CO_3 (carbonic acid) isomeric to it.

We follow Bader's atoms in molecule (AIM) approach [42] and its extensions [43–48] implemented in Gaussian package [41]: in the AIM approach, the strength of a chemical bond and its bond order are reflected in the electron density $\rho(\vec{r}_c)$ at the bond critical point (bcp) $\vec{r}_c$ (i.e., a point where $\vec{\nabla}\rho(\vec{r})$ vanishes) and its Laplacian $\nabla^2\rho(\vec{r}_c)$ (hence the curvatures of the density hyper-surfaces) at bcp. The 0.040 a.u. electric field actually marks the onset of an exotic *field-induced molecular bond* between the C and O′ atoms, having covalent-like attributes, as established below. AIM analysis [42–48] deems that a negative-valued Laplacian of the electron density at the bcp signifies a covalent-type bonding process. Table 3, in conformity with this fact makes it evident that although the C and O′ atoms get sufficiently close (1.781 Å) for the 0.040 a.u. field, the actual bond formation takes place at 0.044 a.u. and above. Table 3 reveals a significant increase in charge density at the critical point of the CO′ bond for the field strength of 0.042 a.u.; the Laplacian still remaining positive. The latter becomes negative for field values of 0.044 a.u. onward, consummating the covalent-like strong bond formation due to the intervening electron density being shared between the C and O′ atoms. Variation in the Laplacian of the electron density as a function of field strength at the critical point between the C and O′ bonding atoms is displayed in Fig. 2.

Interestingly, natural-bond-orbital (NBO) population analysis shows that increasing field strength reduces mostly the '*p*' character on the carbon atom (from 82 to 65%) with simultaneous enhancement in its '*s*' character (18–34%). Atomic orbital occupancies corresponding to the C–O′ bonding were observed only for $F \geq 0.044$ a.u. It is noteworthy from Table 3 that values of the electron densities (in a.u., $1/a_o^3$) at bcp's at zero field changed over ($\rightarrow$) to those at the 0.098 a.u. field respectively are: CO bond: 0.463 $\rightarrow$ 0.379; OH bond: 0.373 $\rightarrow$ 0.245; and for the C–O′ bond: 0.008 $\rightarrow$ 0.250. This brings out the fact that for the CO and OH bonds, there is depletion of electron density, while for the C–O′ bond there is accumulation *over 31 times* its field-free value, the 'build-up' endowing the C–O′ bond a covalent-like character. Another remarkable effect, viz. an O–C=O $\leftrightarrow$ O=C–O resonance is concomitantly seen to occur in the CO_2 moiety of the complex, once the C and O′ atoms get strongly bonded together. The charge densities at bcp on both the CO bonds of carbon dioxide always remain equal for a given electric field (for instance, 0.236 a.u for field strength of 0.080 a.u.) and it is this C–O bond resonance between the arms of the CO_2 subunit that restores the valence of four for the ubiquitously tetravalent carbon atom. Figure 1 schematically depicts this stimulated covalent-like bonding process.

It was, however, demonstrated that a careful selection of functionals is required for the description of non-covalent systems [49–52]. Among different GGA and hybrid functionals, PBE1PBE functional is found to consistently provide decent results, for e.g., interaction energy, geometry, etc. in many non-covalent interacting systems. A detailed account of C O′ distance, density $\rho(\vec{r}_c)$ at bcp, Laplacian of density $\nabla^2\rho(\vec{r}_c)$ and interaction energy (ΔE) calculated at different level of theory employing the 6–311++G(2d,2p) basis set is presented in Tables 4, 5 and 6. Interestingly, all methods employed lead to the 'field-induced covalence' (C–O′), except for minor shifts in numbers, which conclusively establishes that induction of bonding is a major

Table 3 Charge density $\rho(e/a_o^3)$and its Laplacian $\nabla^2\rho(e/a_o^5)$ (in a.u.) in the $H_2O'{\cdot}CO_2$ complex, at the corresponding bond critical points calculated through B3LYP density functional method

Electric field (in a.u.)	ρ (CO) (a.u.)	$\nabla^2\rho$ (CO) (a.u.)	ρ (O′H) (a.u.)	$\nabla^2\rho$ (O′H) (a.u.)	ρ (C·O′) (a.u.)	$\nabla^2\rho$ (C·O′) (a.u.)
0.000	0.463	–0.252	0.373	–2.714	0.008	0.037
0.010	0.463	–0.258	0.371	–2.724	0.011	0.046
0.020	0.462	–0.272	0.368	–2.728	0.015	0.059
0.030	0.459	–0.308	0.363	–2.731	0.024	0.084
0.038	0.443	–0.471	0.353	–2.740	0.071	0.147
0.040	0.434	–0.579	0.347	–2.737	0.105	0.114
0.042	0.428	–0.647	0.343	–2.726	0.128	0.051
0.044	0.425	–0.691	0.340	–2.715	0.143	–0.008
0.046	0.422	–0.724	0.337	–2.705	0.155	–0.063
0.048	0.419	–0.750	0.334	–2.693	0.164	–0.113
0.050	0.417	–0.773	0.332	–2.683	0.172	–0.161
0.060	0.407	–0.852	0.319	–2.605	0.201	–0.342
0.070	0.399	–0.905	0.304	–2.509	0.221	–0.475
0.080	0.391	–0.943	0.287	–2.384	0.236	–0.572
0.090	0.383	–0.964	0.266	–2.220	0.247	–0.632
0.098	0.379	–0.964	0.245	–2.045	0.250	–0.636

After the value of $F = 0.044$ a.u., the Laplacian is negative signifying covalence

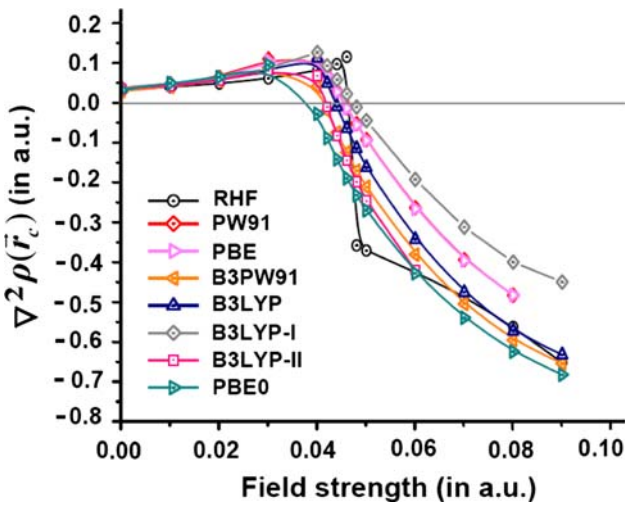

Fig. 2 Laplacian of the electron density ($\nabla^2\rho(\vec{r}_c)$ in a.u.) as a function of field strength at the critical point between the C and O′ bonding atoms in the planar $H_2O'{\cdot}CO_2$ complex, calculated at different level of theory employing the 6–311++G(2d,2p) basis set. PW91 = PW91PW91, PBE = PBEPBE, PBE0 = PBE1PBE, B3LYP-I = B3LYP/aug-cc-pVDZ, B3LYP-II = B3LYP/aug-cc-pVTZ

effect, and is neither an artifact of the level of computation, nor the exchange-correlation functional used. The fields at which C–O′ covalent-like bond formation take place, as indicated by negative Lapalacian of density at critical point between the C and O′ bonding atoms, at different levels of theory lie in the range (0.040–0.048 a.u.). It is evident from the tables that the variations of C–O′ distance, the charge density and Laplacian with applied field predicted at the B3LYP level are consistent with those at PBE1PBE and other functionals. Estimation of interaction energy ΔE at the 0.098 a.u. field strength yields as follows: (RHF: -168.18 kcal mol^{-1}), (B3PW91: -172.20 kcal mol^{-1}), (B3LYP: -171.99 kcal mol^{-1}) and (PBE1PBE1: -174.98 kcal mol^{-1}). Thus B3LYP level, one of the levels of theory under which a full optimization of structures is possible, is seen to provide a decent description for field effects on the otherwise weakly bound $H_2O'{\cdot}CO_2$ complex. Since the applied field builds up considerable intervening electron density shared between the C and O′ atoms, the complex in the presence of field no longer remains 'weakly' bound. We shall continue with the B3LYP description on the field effects on vibrational spectra (which we present shortly) along with the frequency values calculated employing the PBE1PBE functional with the same basis set, 6–311++G(2d,2p).

Classically, when the electric field is applied to a species with the electric dipole moment $\vec{\mu}$, due to the $-\vec{\mu}\cdot\vec{F}$ interaction, the dipole moment gets favorably aligned along the field $\vec{F}$. Seen from another standpoint, the field exerts a torque $\vec{\mu}\times\vec{F}$, leading to the alignment. For the present system of carbon-dioxide and water, the net electric dipole moment is directed from the C atom toward the O′ atom, owing to preponderance of negative charge in the dioxide segment, and its deficit around the hydrogens of water. Meanwhile, the carbon atom, by itself, is more electropositive relative to the oxygen O′. A peculiar situation now arises owing to two competing processes: the negative charge density tends to migrate from the region

Table 4 Field free and field present C–O′ distance, density $\rho(\vec{r}_c)$ at bcp, Laplacian of density $\nabla^2\rho(\vec{r}_c)$ and interaction energy (ΔE) calculated at different level of theory employing the 6–311++G(2d,2p) basis set

Method	Field free C–O′ dist. (Å)	Field[a] free ΔE (kcal mol^{-1})	Field free $\rho(\vec{r}_c)$ (a.u.)	Field[a] F (a.u.)	C–O′ length at F (Å)	$\rho(\vec{r}_c)$ at F (a.u.)	$\nabla^2\rho(\vec{r}_c)$ at F (a.u.)	ΔE at F (kcal mol^{-1})	F^{b}_{Max} (a.u.)	C–O′ length at F_{Max} (Å)
HF	2.919	–2.09	0.005	0.048[e]	1.494	0.198	–0.357	–56.67	0.120	1.383
MP2	2.803	–2.72	0.008							
GGA										
PW91PW91	2.846	–2.43	0.009	0.046[f]	1.643	0.148	–0.010	–48.47	0.080	1.470
PBEPBE	2.873	–2.09	0.008	0.046[f]	1.643	0.149	–0.012	–47.90	0.080	1.471
Hybrid										
B3PW91	2.950	–1.23	0.007	0.042[e]	1.644	0.146	–0.018	–39.77	0.098	1.436
B3LYP	2.867	–1.90	0.008	0.044[e]	1.652	0.143	–0.008	–41.47	0.098	1.442
B3LYP-I[c]	2.848	–1.94	0.008	0.048[f]	1.595	0.163	–0.009	–52.25	0.090	1.452
B3LYP-II[d]	2.867	–1.78	0.008	0.042[f]	1.708	0.130	–0.009	–35.54	0.060	1.514
PBE1PBE	2.812	–2.30	0.008	0.040[e]	1.638	0.147	–0.026	–39.48	0.110	1.462

[a] Field at which C–O′ bond forms

[b] Maximum applied field

[c] B3LYP-I = B3LYP/aug-cc-pVDZ

[d] B3LYP-II = B3LYP/aug-cc-pVTZ

[e] Orbital occupancies (as revealed by the NBO population analysis) corresponding to the C–O′ bonding start at the same field value

[f] Orbital occupancies start at 0.044 a.u

Table 5 Distance (in Å) between the C and O′ bonding atoms in the planar $H_2O'\cdot CO_2$ complex calculated at different level of theory employing the 6–311++G(2d,2p) basis set

Electric field (in a.u.)	C–O′ separation (in Å)							
	RHF	PW91	PBE	B3PW91	B3LYP	B3LYP-I	B3LYP-II	PBE0
0.000	2.919	2.846	2.873	2.950	2.867	2.848	2.867	2.812
0.010	2.821	2.723	2.744	2.793	2.754	2.734	2.752	2.704
0.020	2.712	2.552	2.576	2.623	2.613	2.597	2.611	2.565
0.030	2.587	2.231	2.258	2.367	2.401	2.383	2.401	2.332
0.040	2.414	1.761	1.761	1.688	1.781	1.734	1.794	1.638
0.042	2.364	1.710	1.710	1.644	1.700	1.681	1.708	1.606
0.044	2.298	1.673	1.673	1.613	1.652	1.644	1.658	1.582
0.046	2.137	1.643	1.643	1.590	1.620	1.616	1.624	1.564
0.048	1.494	1.619	1.619	1.571	1.595	1.595	1.599	1.548
0.050	1.485	1.599	1.599	1.555	1.576	1.576	1.578	1.536
0.060	1.452	1.532	1.533	1.503	1.516	1.517	1.514	1.489
0.070	1.429	1.493	1.494	1.470	1.480	1.482	–	1.460
0.080	1.412	1.470	1.471	1.448	1.457	1.461	–	1.440
0.090	1.398	–	–	1.436	1.443	1.451	–	1.429
0.100	1.388	–	–	–	–	–	–	1.427
0.110	1.381	–	–	–	–	–	–	1.462
0.120	1.383	–	–	–	–	–	–	–

PW91 = PW91PW91, PBE = PBEPBE, PBE0 = PBE1PBE, B3LYP-I = B3LYP/aug-cc-pVDZ, B3LYP-II = B3LYP/aug-cc-pVTZ

Table 6 Electron density $\rho(a_o^{-3})$ (in a.u.) at the critical point between the C and O′ bonding atoms in the planar $H_2O'{\cdot}CO_2$ complex calculated at different level of theory employing the 6–311++G(2d,2p) basis set

Electric field (in a.u.)	Electron density $\rho(\vec{r}_c)$ (in a.u.)							
	RHF	PW91	PBE	B3PW91	B3LYP	B3LYP-I	B3LYP-II	PBE0
0.000	0.005	0.009	0.008	0.007	0.008	0.008	0.008	0.008
0.010	0.008	0.012	0.011	0.010	0.011	0.011	0.011	0.012
0.020	0.011	0.018	0.017	0.014	0.015	0.015	0.015	0.016
0.030	0.014	0.037	0.035	0.026	0.024	0.026	0.024	0.028
0.040	0.021	0.112	0.112	0.131	0.105	0.117	0.106	0.147
0.042	0.024	0.127	0.127	0.146	0.128	0.133	0.130	0.159
0.044	0.028	0.138	0.139	0.157	0.143	0.145	0.146	0.168
0.046	0.038	0.148	0.149	0.166	0.155	0.155	0.158	0.176
0.048	0.198	0.157	0.158	0.174	0.164	0.163	0.168	0.183
0.050	0.204	0.165	0.166	0.181	0.172	0.170	0.177	0.189
0.060	0.224	0.195	0.195	0.207	0.201	0.197	0.207	0.213
0.070	0.241	0.215	0.215	0.226	0.221	0.216	–	0.231
0.080	0.256	0.229	0.229	0.240	0.236	0.229	–	0.244
0.090	0.269	–	–	0.250	0.247	0.238	–	0.254
0.100	0.280	–	–	–	–	–	–	0.258
0.110	0.290	–	–	–	–	–	–	0.240
0.120	0.294	–	–	–	–	–	–	–

PW91 = PW91PW91, PBE = PBEPBE, PBE0 = PBE1PBE, B3LYP-I = B3LYP/aug-cc-pVDZ, B3LYP-II = B3LYP/aug-cc-pVTZ

around the dioxide-oxygens, i.e. from around the electropositive C toward the electronegative O′. However, the electric field being directed from C to O′, electric potential associated with the applied field is (relatively) negative around O′, which tends to inhibit a negative charge build-up in its proximity; consequently, the negative charge gets 'arrested' midway. In addition, the field direction is also conducive for the C and O′ atoms to move toward each other, which accounts for the compression of the C–O′ bond. Mulliken charges (Table 7) on the constituent atoms manifestly unravel the charge-transfer process: both the positive (Mulliken) charge on C and the negative charge on O′ first tend to enhance in magnitude, but subsequently diminish, to almost neutrality around the field of 0.82–0.84 a.u.; further with 'overcompensation' for C, lending it a negative charge. Starting from the zero-field value, the relatively electropositive C atom is rendered negatively charged; with the charge on the relatively electronegative O′ almost neutralized at the 0.098 a.u. field. Application of the field thus results in a net migration of electrons in the region amidst the C and O′ atoms, with a compression in their inter-atomic spacing, endowing the bond between them a covalent-like character. Table 7 also brings out the perfect equivalence of the two oxygens of CO_2 as deemed by their resonance; along with complete equivalence of the two hydrogens of H_2O. Thus the exotic C–O′ bond that exhibits a covalent–like character, in terms of sharing of the electron density, is accompanied by a charge-transfer, imparting the carbon atom a substantial *negative* charge with a substantial electron deficiency at the oxygen O′ site.

The enhanced bonding between C and O′ atoms in the $H_2O'{\cdot}CO_2$ complex must leave its imprint on the vibrational response: field-free and field-perturbed IR and Raman spectra for the complex with regards to O′H stretch, asymmetric CO-stretch and C–O′ stretch are presented in Table 8. The field-free frequencies calculated at the high-level ab initio theory [35], viz., MP2/aug-cc-pVTZ and the experimental frequencies (for a complex trapped in a nitrogen matrix) [35] are presented for comparison with the present calculation. The calculated field-free frequencies are in agreement with those obtained at MP2/aug-cc-pVTZ level except for small shift in the range ($\sim$10 to $\sim$20 cm^{-1}). The frequencies calculated through the PBE1PBE/6–311++G(2d,2p) method are presented in Table 9. It is evident from the tables that the variation in the vibrational frequencies as a function of applied field obtained through B3LYP/6–311++G(2d,2p) is consistent with PBE1PBE/6–311++G(2d,2p) calculations throughout the range of applied field strength, 0–0.098 a.u. We describe herein the field effects in accordance with B3LYP level.

The two field-free vibrational bands centered at 3,821 and 3,924 cm^{-1}, respectively, correspond to the symmetric and antisymmetric O′H stretches, whose intensities get

Table 7 Mulliken charge q_X, of the constituent atom "X" as a function of the applied electric field calculated at B3LYP/6–311++G(2d,2p) level of theory

Field a.u.	O1 $q_{O1\text{-dioxide}}$	O2 $q_{O2\text{-dioxide}}$	C q_C	O′ $q_{O'}$	H1 $q_{H1\text{-water}}$	H2 $q_{H2\text{-water}}$
0.000	–0.227709	−0.227709	0.451112	−0.495648	0.249977	0.249977
0.010	−0.236746	−0.236746	0.451892	−0.530469	0.276035	0.276035
0.020	−0.252463	−0.252463	0.456152	−0.556711	0.302742	0.302742
0.030	−0.287701	−0.287701	0.468636	−0.556923	0.331845	0.331845
0.036	−0.357588	−0.357588	0.494863	−0.491818	0.356066	0.356066
0.038	−0.420010	−0.420010	0.520987	−0.420640	0.369837	0.369837
0.040	−0.489235	−0.489235	0.555280	−0.345926	0.384558	0.384558
0.042	−0.526623	−0.526623	0.572531	−0.308129	0.394422	0.394422
0.044	−0.550364	−0.550364	0.580382	−0.284563	0.402454	0.402454
0.046	−0.566944	−0.566944	0.582276	−0.266840	0.409226	0.409226
0.048	−0.580298	−0.580298	0.581095	−0.252191	0.415847	0.415847
0.050	−0.590188	−0.590188	0.576461	−0.240003	0.421959	0.421959
0.060	−0.615771	−0.615771	0.517740	−0.192590	0.453195	0.453195
0.070	−0.600852	−0.600852	0.378987	−0.151279	0.486998	0.486998
0.080	−0.526046	−0.526046	0.111552	−0.111603	0.526071	0.526071
0.082	−0.501559	−0.501559	0.038168	−0.104190	0.534570	0.534570
0.084	−0.473461	−0.473461	−0.042471	−0.097119	0.543255	0.543255
0.086	−0.441933	−0.441933	−0.129844	−0.090646	0.552178	0.552178
0.088	−0.406916	−0.406916	−0.224039	−0.085122	0.561497	0.561497
0.090	−0.368147	−0.368147	−0.324887	−0.079802	0.570492	0.570492
0.098	−0.179616	−0.179616	−0.786654	−0.072745	0.609316	0.609316

enhanced with a 'red shift' with increasing applied field. For low fields, the C–O′ stretching mode is IR as well as Raman inactive (Table 5). It becomes IR active and manifests at 317 cm^{-1} (for field of 0.044 a.u.) only after the 'covalence' onset threshold of 0.040 a.u. field, and subsequently starts to exhibit increasing Raman activity. Insignificance of IR intensity and Raman activity for $F < 0.040$ a.u., ranks the field of 0.040 a.u. as the onset for enhanced bonding between the two molecules that behave akin to a single molecular species up to field of 0.098 a.u. Intensity of CO stretching band gets enhanced with the field and shifts toward lower frequency, and at high fields ($F > 0.070$ a.u.), while its IR intensity diminishes, the asymmetric CO stretching vibration becomes increasingly Raman active, most prominently so for the 0.090 a.u. field.

3 Conclusions

In summary, the external electric field polarizes CO_2, the non-polar subunit, enhancing its dipole–dipole interaction with H_2O; consequently, the molecules get closer with considerable enhancement in bonding and lowering of the total energy. It must be noted that major change in the energy is associated with the dipolar interactions with the external field, which is further accentuated by mutual polarization in response to it. Remarkably, the $H_2O'{\cdot}CO_2$ complex shows an increasingly stable, strong covalent-like C–O′ bond induced by the field strength between 0.044 and 0.098 a.u.; ratified by the density topography. For electric field strength above 0.098 a.u., the geometry of the system gets distorted and eventually slips into a transition state (TS) characterized by one imaginary vibrational frequency on its potential energy surface (PES). Up till this 'threshold' field, the system exhibits stable bound states borne out by strong local minima on the PES for field values in the range 0 a.u. → 0.098 a.u.; with an emergence of covalent-like C–O′ bond at the field strength of 0.044 a.u., which increases in its strength up to the threshold. Beyond the threshold, the nuclear repulsion dominates and the complex tends to dissociate, as noted above.

Very strong fields far beyond 0.098 a.u., however, distort even the TS structure to the extent that geometry optimization fails to converge, indicating dissociation, or possibly a dissociative ionization which is actually discernible with a time-harmonic 'dynamic' laser field within the realm of time-dependent perturbation theory, applied to laser–molecule interactions [30, 31]. Its analogous

Table 8 Calculated vibrational frequencies (in cm^{-1}) as a function of applied field strength in the planar $H_2O'{\cdot}CO_2$ complex at the B3LYP/6–311++G(2d,2p) level of theory; respective IR intensities ($km\ mol^{-1}$) are given in the first parentheses and the Raman activity ($Å^4\ amu^{-1}$) in second parentheses

Vibrational modes	Electric field (in a.u.)									
	0.000	0.010	0.020	0.030	0.040	0.044	0.060	0.080	0.090	0.098
C–O′ stretching	92	107	126	144	187	317	532	586	585	576
	(0)	(0)	(5)	(15)	(160)	(133)	(6)	(0)	(0)	(0)
	(0)	(0)	(0)	(0)	(0)	(3)	(5)	(32)	(31)	(43)
	107[a]									
CO_2 bending	664	653	632	594	653	690	767	841	846	813
(in the plane)	(46)	(56)	(78)	(141)	(250)	(252)	(209)	(29)	(0)	(43)
	(0)	(0)	(5)	(14)	(0)	(0)	(35)	(343)	(529)	(751)
	650[a]									
	656[b]									
CO_2 bending	678	678	679	686	734	758	790	815	814	791
(out of plane)	(29)	(28)	(25)	(16)	(5)	(4)	(0)	(34)	(82)	(9)
	(0)	(0)	(0)	(0)	(0)	(0)	(0)	(74)	(267)	(409)
	663[a]									
	665[b]									
Symmetric CO stretching	1,364	1,363	1,359	1,348	1,300	1,293	1,289	1,268	1,230	1,175
	(0)	(0)	(5)	(23)	(172)	(220)	(320)	(278)	(136)	(41)
	(18)	(20)	(24)	(36)	(25)	(21)	(17)	(245)	(585)	(652)
	1,328[a]									
	1,277[b]									
HO′H bending (scissor motion of H_2O)	1,637	1,660	1,680	1,687	1,653	1,654	1,666	1,657	1,638	1,605
	(75)	(78)	(76)	(65)	(122)	(164)	(221)	(236)	(267)	(384)
	(0)	(0)	(0)	(6)	(0)	(0)	(0)	(14)	(5)	(12)
	1,627[a]									
	1,598[b]									
Asymmetric CO stretching	2 400	2,394	2,378	2,333	2,028	1,924	1,736	1,389	998	871
	(656)	(663)	(678)	(710)	(825)	(839)	(817)	(434)	(57)	(7)
	(0)	(0)	(0)	(0)	(6)	(4)	(0)	(1,818)	(3,980)	(493)
	2,404[a]									
	2,351[b]									
Symmetric O′H stretching	3,821	3,809	3,787	3,752	3,628	3,565	3,378	3,068	2,845	2,612
	(10)	(26)	(54)	(118)	(346)	(414)	(699)	(1,455)	(2,142)	(2,804)
	(84)	(83)	(93)	(135)	(149)	(140)	(211)	(692)	(793)	(716)
	3,820[a]									
	3,631[b]									
Asymmetric O′H stretching	3,924	3,897	3,861	3,817	3,719	3,655	3,440	3,088	2,838	2,577
	(72)	(93)	(118)	(115)	(314)	(378)	(522)	(623)	(574)	(550)
	(27)	(26)	(26)	(28)	(29)	(28)	(23)	(0)	(48)	(5)
	3,944[a]									
	3,724[b]									

[a] Calculated at MP2/aug-cc-pVTZ level [35]

[b] Experimental value (complex trapped in a nitrogen matrix) [35]

'signature' in the present *static* case on the other hand, is just its failure to converge to a local minimum. Although it is beyond the scope of the present work, we suggest that an experimental verification of the proposition made herein could come through a scanning tunneling apparatus with adsorbed carbon-dioxide and water vapor [53] at sub-

Table 9 Vibrational frequencies (in cm^{-1}) of the planar $H_2O'{\cdot}CO_2$ complex calculated at the PBE1PBE/6–311++G(2d,2p) level of theory

Vibrational modes	Electric Field (in a.u.)									
	0.000	0.010	0.020	0.030	0.040	0.044	0.060	0.080	0.090	0.098
C–O′ stretching	96 (0)	114 (0)	131 (5)	144 (22)	322 (139)	418 (87)	572 (5)	604 (0)	597 (0)	590 (0)
CO_2 bending (in the plane)	674 (47)	662 (58)	639 (82)	598 (150)	695 (249)	717 (258)	801 (197)	878 (23)	881 (0)	862 (47)
CO_2 bending (out of plane)	690 (28)	690 (28)	690 (25)	693 (16)	769 (6)	781 (5)	806 (0)	828 (25)	831 (82)	807 (5)
Symmetric CO stretching	1,386 (0)	1,386 (0)	1,382 (6)	1,369 (26)	1,321 (202)	1,323 (234)	1,325 (325)	1,313 (288)	1,276 (131)	1,221 (35)
HO′H bending (scissor motion of H_2O)	1,642 (76)	1,667 (79)	1,685 (78)	1,692 (69)	1,657 (176)	1,662 (198)	1,676 (246)	1,669 (250)	1,652 (261)	1,625 (265)
Asymmetric CO stretching	2,444 (666)	2,438 (674)	2,422 (689)	2,370 (724)	1,992 (838)	1,934 (840)	1,782 (825)	1,470 (500)	1,028 (55)	891 (5)
Symmetric O′H stretching	3,882 (12)	3,866 (28)	3,844 (58)	3,807 (124)	3,649 (361)	3,602 (416)	3,431 (679)	3,131 (1,421)	2,907 (2,147)	2,683 (2,816)
Asymmetric O′H stretching	3,990 (78)	3,959 (98)	3,924 (124)	3,879 (164)	3,749 (367)	3,696 (408)	3,496 (533)	3,154 (636)	2,904 (569)	2,652 (528)

Value in the parenthesis is IR intensity (km mol^{-1})

liquid-helium temperatures. To conclude, we believe that the answer to the interrogation in the title is completely vindicated in the affirmative: that an external electric field applied to certain specific weakly bound polar–non-polar complexes can induce enhanced, exotic, covalent-like bonding.

Acknowledgments D.R. thanks HRDD under the State Government of Sikkim, India, for study-leave. S.P.G acknowledges the research grant from the University of Pune through the 'University Potential for Excellence' Research Scheme. R.K.P. gratefully acknowledges the Financial Support from Research Grant UPE/BCUD/RG/09, by the University of Pune, India. Discussions with Professor Dr. Chandrakant Dharmadhikari (Pune), both on high electric fields on the atomic scale and also on a possible experimental realization of the present work (with cold nano-tips in a scanning tunneling apparatus) are gratefully acknowledged. Finally, R.K.P. would like to thank Professor Dr. Joseph Dannenberg for a stimulating discussion in New York City this March on this exotic theme.

References

1. Nesbitt DJ (1988) Chem Rev 88:843 2
2. Nesbitt DJ, Lovejoy CM (1992) J Chem Phys 96:5712 3
3. Sapse AM (1983) J Chem Phys 78:5733
4. Rice JK, Coudert LH, Mastsumura K, Suenram RD, Lovas F, Stahl JW, Pauley DJ, Kukolich SG (1990) J Chem Phys 92:6408
5. Baiocchi FA, Dixon TA, Joyner CH, Klemperer W (1981) J Chem Phys 74:6544
6. Block M, Marshall D, Pedersen LG, Miller RE (1992) J Chem Phys 96:7321
7. Scheiner S (1997) Hydrogen bonding: a theoretical perspective. Oxford University Press, New York
8. Tzeli D, Mavridis A, Xantheas SS (2002) J Phys Chem A 106:11327
9. Rozas I, Alkorta I, Elguero J (1997) Chem Phys Lett 275:423
10. Jordan MJT, Thompson KC (2003) Chem Phys Lett 370:14
11. Jordan MJT, Bene JED (2000) J Am Chem Soc 122:2101
12. Jetti RKR, Boese R, Thakur TS, Vangalab VR, Desiraju GR (2004) Chem Comm 2526–2527
13. Iannuzzi M, Parrinello M (2004) Phys Rev Lett 93:025901
14. Fontaine-Vive F, Johnson MR, Kearley GJ, Cowan JA, Howard JAK, Parker SF (2006) J Chem Phys 124:234503
15. Choi YC, Kim WY, Park KS, Tarakeshwar P, Kim KS, Kim TS (2005) J Chem Phys 122:094706
16. Remacle R, Willner I, Levine RD (2004) J Phys Chem B 108:18129
17. Delaney P, Nolan M, Greer JC (2005) J Chem Phys 122:044710
18. Remacle R, Levine RD (2006) Faraday Discuss 131:45
19. De Lara EC, Kahn R, Seloudoux R (1985) J Chem Phys 83:2646
20. Kriegl JM, Nienhaus K, Deng P, Fuchs J, Nienhaus GU (2003) Proc Natl Acad Sci USA 100:7069
21. Lehle H, Kriegl JM, Nienhaus K, Deng P, Fengler S, Nienhaus GU (2005) Biophys J 88:1978
22. Suydam IT, Snow CD, Pande VS, Boxer SG (2006) Science 313:200
23. Dharmadhikari CV (2000) Scanning tunneling microscopy/spectroscopy of surfaces. In: Meyers RA (ed) Encyclopedia of analytical chemistry. Wiley, Chinchester, pp 9284–9301
24. Park ES, Andrews SS, Hu RB, Boxer SG (1999) J Phys Chem B 103:9813
25. Park ES, Thomas MR, Boxer SG (2000) J Am Chem Soc 122:12297

26. Suydam IT, Boxer SG (2003) Biochemistry 42:12050
27. Rai D, Joshi H, Kulkarni AD, Gejji SP, Pathak RK (2007) J Phys Chem A 111:9111 (and references therein)
28. James TD, Wales J, Rozas JH (2007) J Chem Phys 126:054506 (and references therein)
29. Rai D, Kulkarni AD, Gejji SP, Pathak RK (2008) J Chem Phys 128:034310
30. Bandrauk AD, Sedik E-WS, Matta CF (2004) J Chem Phys 121:7764
31. Kawai S, Bandrauk AD, Jaffé C, Bartsch T, Palacián J, Uzer T (2007) J Chem Phys 126:164306
32. Matta I, Molins E, Alkorta I, Espinosa E (2009) J Chem Phys 130:044104
33. Peterson KI, Klemperer W (1984) J Chem Phys 80:2439
34. Makarewicz J, Ha TK, Bauder A (1993) J Chem Phys 99:3694
35. Schriver A, Schriver-Mazzuoli L, Chaquin P, Dumont E (2006) J Phys Chem A 110:51
36. Yoo CS, Iota V, Cynn H (2001) Phys Rev Lett 86:444
37. Park JH, Yoo CS, Iota V, Cynn H, Nicol MF, Le Bihan T (2003) Phys Rev B 68:014107
38. Tassone F, Chiarotti GL, Rousseau R, Scandolo S, Tosatti E (2005) Chem Phys Chem 6:1752
39. Becke AD (1993) J Chem Phys 98:5648
40. Lee C, Yang W, Parr RG (1988) Phys Rev B 37:785
41. Frisch MJ et al (2004) Gaussian 03, Revision C.02. Gaussian, Inc., Wallingford
42. Bader RFW (1994) Atoms in molecules: a quantum theory. Oxford University Press, Oxford
43. Cioslowski J (1992) Chem Phys Lett 194:73
44. Cioslowski J (1994) Chem Phys Lett 219:151
45. Cioslowski J, Nanayakkara A, Challacombe M (1993) Chem Phys Lett 203:137
46. Cioslowski J, Stefanov BB (1995) Mol Phys 84:707
47. Stefanov BB, Cioslowski J (1995) J Comput Chem 16:1394
48. Matta CF, Boyd RJ (eds) (2007) An introduction to the quantum theory of atoms in molecules. Wiley, New York, pp 251–252
49. Subramanina V, Sivanesan D, Padmanabhan J, Lakshminarayanan N, Ramasami T (1999) Proc Indian Acad Sci (Chem Sci) 111:369
50. Xu X, Goddard WAIII (2003) Proc Natl Acad Sci USA 101:2673
51. Alemán C, Curcó D, Casanovas J (2005) Phys Rev E 72:026704
52. Croft AK, Howard-Jones HM (2007) Phys Chem Chem Phys 9:5649
53. Dharmadhikari CV (in a private communication to R.K.P.)